A Review of Manufacturing Materials and Production Methods for Frequency-Selective Structures

David Ferreira, Rafael F. S. Caldeirinha, Iñigo Cuiñas, and Telmo R. Fernandes

This article presents a review of frequency-selective structure (FSS) manufacturing materials and production methods ranging from the common printed circuit board (PCB)-based designs to textile, ink, metal, or fluid prototypes. Our work gathers some of the most relevant solutions published by the scientific community and considers several examples depicted for each case. Additionally, the main physical parameters that may have a significant impact on FSS performance have been identified, e.g., electrical conductivity of the FSS conductive element and the relative permittivity and thickness of the FSS dielectric material. Finally, a comparative analysis of the materials and techniques is presented, which highlights the benefits and limitations of each solution.

EDITOR'S NOTE

Eva Rajo-Iglesias

This issue's "Wireless Corner" column presents a complete review of frequency-selective structure (FSS) manufacturing techniques. The varied possibilities, from classic printed circuit boards to more advanced options such as readily available textile or fluid prototypes, are discussed by showing several examples available in current literature. The impact of the conductivity, dielectric permittivity, and thickness in FSS performance is also discussed. Finally, a comparison of the different techniques in terms of relevant metrics such as approximate cost, tuning possibility, mechanical flexibility, and electrical conductivity is provided.

DESIGN OF FSSs

FSSs are periodic arrays of unit cells, which can be either thin sheets [quasi-two-dimensional (2-D) surfaces] or three-dimensional (3-D) elements that, as the name suggests, exhibit specific frequency selectivity for impinging electromagnetic (EM) waves. These structures have evolved considerably in their design, complexity, and performance since the 1960s [1]. However, in 1956, a partially reflective surface made with a dichroic filter was introduced by Trentini [2]. This evolution has been used in military and commercial applications, two fields that are continuously developing wireless technology. The improvement in analytical methods and availability of full-wave-solver software solutions, coupled with nonstop increasing computational power, allowed researchers to study and propose many different FSS designs by varying their unit-cell complexity or manufacturing materials. Typical FSS applications include, but are not limited to, spatial/angular filters in indoor environments, radomes, dichroic filters, or artificial beamsteering [1]–[13].

Whether for laboratory proof-of-concept assessment or for large quantities as a commercial solution, including the environment for which the FSS is intended, there are numerous criteria that may dictate the FSS source material and, consequently, the manufacturing method. This article provides an overview of this topic based on several journal and conference publications, highlighting the main benefits and limitations of each material and production method.

FSS MATERIALS

FSSs can be manufactured using different materials and, for some, multiple manufacturing techniques may be

Digital Object Identifier 10.1109/MAP.2018.2870583
Date of publication: 29 November 2018

available. This review focuses only on "ready-to-use" materials, i.e., products that may be manufactured from the combination of different source/raw elements. With this definition in mind, five main categories were considered: PCBs, ink, textiles, metal, and fluids.

PCBs

PCBs are manufactured by several companies with diverse compositions that yield different mechanical, electrical, and thermal properties. Many scientific publications use PCBs to manufacture and measure different FSS prototypes, such as in [14]–[45]. A PCB consists of copper sheets laminated onto a nonelectrically conductive substrate and, depending on its application, may be single sided (one copper sheet), double sided (two copper sheets at both sides of a single substrate), or multilayered (multiple substrate and copper layers). The desired pattern may then be obtained from the copper-panelized PCB with a subtractive method, more specifically through milling, laser ablation, or, more commonly, by etching chemical procedures.

FSSs are typically single [29], [34], [35], [37], [39] or double sided [14], [26]–[28], [33], [35], [38], [44], with some authors assembling multilayer FSSs [30], [35], [36], [40], [42], [43], [45], which consist of single- or double-sided boards spaced by an air gap or substrate. The latter boards are usually chosen to increase the FSS frequency roll-off factor or to combine different frequency responses for a specific multiband behavior. Examples of FSS prototypes are illustrated in Figure 1.

In relation to flexible PCB substrates, there is a range of substrates used for FSSs, including Mylar (sometimes referred to as *polyester films*) [14], [15] and RO3003 [16]. They can be very inexpensive on a per-cell basis and offer low transmission losses and increased flexibility [15], [16].

A passive FSS frequency response may be significantly modified, either once in the assembling stage or, for switching/tuning capability, by including discrete components within the unit cells. In a fixed-frequency response FSS scenario, surface-mount device capacitors may be used, while, for active FSSs (e.g., controlled through applied voltage bias), p-i-n diodes [26], [28], [29], [31] or varactors [24], [32] may be soldered to the PCB. Consequently, some authors devise the bias grid on the same layer as the FSS, while others may use an additional layer for such a purpose.

The aforementioned FSSs are commonly referred to as *frequency-selective surfaces* or *2-D FSSs* since they are formed from very thin sheets of copper and substrate. A different approach involves arranging multiple PCB sheets, resulting in a 3-D FSS [35], [36], [41]. These structures are usually chosen for improved frequency response and angular-incidence stability, as shown in Figure 1(d).

INK

Electrically conductive ink has also been used by several authors as an alternative approach to manufacture FSSs [46]–[55]. In fact, some methods perform adequately even when flexible textile substrates are used [55]. Metal nanoparticle-based inks allow the use of different substrates such as paper [46], glass [50], [54], various polyester materials, e.g., polyethylene naphthalate [48] and polyethylene terephthalate (PET) [49], [51], [52], as well as solid (3-D printed) objects that may be coated with these inks [47]. Excluding the simple method of brush or spray deposition of ink on a solid object like the one performed in [47], additive manufacturing techniques using conductive inks (as opposed to subtractive techniques used with a PCB) can be quite diversified. This is true because of the similarities to radio-frequency identification (RFID) tags and flexible circuit-manufacturing markets, in which various techniques have been proposed, e.g., inkjet printing, lithographic techniques, and roll-to-roll (R2R) printing technologies, the latter of which have high yield and cost-efficiency [49].

A common ink choice in both research and commercial applications is silver nanoparticle ink, which, aside from having the highest conductivity of all metals, is the most readily available in inkjet printable form. Recent developments have enabled stable formulations that provide reproducible print characteristics over a wide range of substrates [46]. Figure 2 depicts some examples of FSSs manufactured with conductive ink.

The authors of [46], [47], and [49] use silver ink as the FSS conductive element with different types of substrates and application methods. In [46], several factors that contributed to the inkjet manufacture of FSSs were investigated when the FSS was printed on a paper

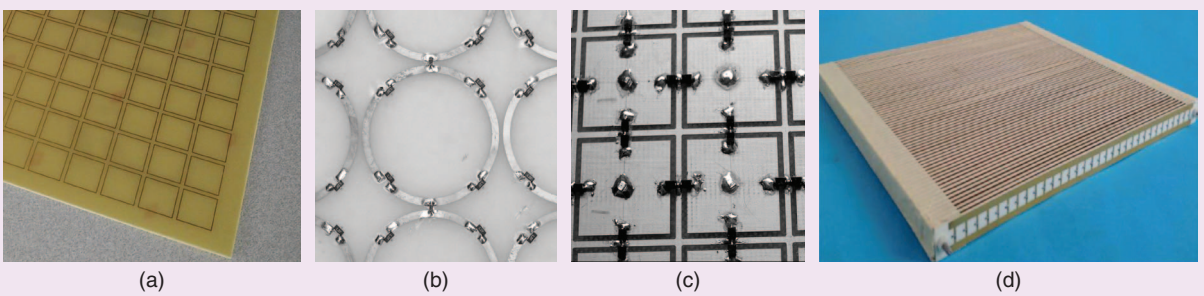

FIGURE 1. Examples of FSSs manufactured from PCB boards. (a) A single-layer passive square loop [37], (b) a single-layer active annular ring [29], (c) a double-layer active square loop [26], and (d) a passive 3-D stepped-impedance resonator [35].

class that contained an inorganic, microporous receiving layer. The number of deposited layers as well as the ability to deposit droplets on demand allowed for modifying the original FSS array element design by reducing the amount of deposited conductive material. The authors concluded that single-layer, thin lines were prone to discontinuities, especially in the case of frame elements, which could be somewhat mitigated by the addition of extra layers of ink. Compared to a PCB-etched FSS, the printed prototype yielded a lower frequency transmission null (associated with different substrate thickness and relative permittivity), with a somewhat similar isolation performance when three layers of conductive ink were applied. In [47], a 3-D proprietary plaster-based material with a vinyl polymer was used to print several FSS elements. These elements were subsequently hand coated with two layers of silver conductive paint. In [48], the authors used a proprietary catalytic ink that, after application on a PET substrate, was subjected to an ultraviolet curing process and then immersed in a solution of copper ions. The ions were deposited on the printed tracks through an autocatalytic deposition process. The implementation of FSS-based chipless RFID tags on a PET foil substrate [49] and a sheet-fed screen-printing machine were used to print the specific patterns on the substrate with a microparticle-based silver paste. In [50], the authors modified the coating procedure of low-emittance glass, thereby allowing the printing of desired patterns on test windows. The soft-coating method is a technique in which very thin metallic oxide layers are deposited on the glass surface in a vacuum chamber to provide high thermal insulation [50].

TEXTILE

Fabric-based FSSs can be seen as yet another alternative approach to conventional FSS materials such as PCBs and were the subject of research in [56]–[61]. Textile-conductive structures have received attention in recent years, partly due to the growing interest in wearable technology as well as on- and off-body communications. These structures offer several advantages, such as light weight, flexibility, and softness [57], [58]. Another benefit associated with this type of FSS is its integration with advanced manufacturing techniques, e.g., computerized knitting [57], embroidery [58], and weaving machines [59]. These machines should be able to provide a consistent output of prescribed geometries for large-scale solutions. Other textile FSS manufacturing techniques are screen printing [59] and hand looming [60]. Finally, other researchers may attempt a hybrid solution by integrating cut-to-shape pieces of commercially available conducting textiles with traditional (nonconducting) fabrics [56] attached with adhesive, stitches, or other means.

For the textile FSS to operate as intended, an appropriate conductive yarn must be carefully chosen. Subsequently, the type of yarn will depend on the manufacturing procedure since it needs to have mechanical properties compatible with the computerized/manual machines. In [57]–[59], different manufacturing techniques (knitting, embroidery, and weaving) were employed and, therefore, compatible yarns for FSS patterning, such as Denier filament polyamide yarn, nylon thread, and Amberstrand fiber were selected. Common to all of these materials is that they were coated or embedded with silver ink to provide electrical conductivity properties.

A few examples of textile-based FSSs are shown in Figure 3. The authors of [57] experimented with knitting two different FSS designs, i.e., grid and patch, for a high- and low-pass frequency-filtering characteristic response. They achieved this prototype using a computerized flat-bed knitting machine. The nonconducting base yarn was polyester and the conducting yarn, with approximately 4-Ω cm, was formed by embedding silver nonparticles on the surface of a 235 Denier 34 filament polyamide 6.6 yarn. The reflectivity measurements demonstrated the expected filtering characteristics, although the authors acknowledged that the conductive-yarn contact mechanics at the contact areas are very complex and their impact on FSS performance was not fully understood. The study in [58] assessed the performance of a textile FSS array manufactured using an embroidery machine. The FSS was fabricated on felt cloth measuring 0.8 mm in thickness, with a 234/34 two-ply, silver-plated, nylon-type thread with 14-Ω ft used as the conductive yarn. The FSS pattern was sewn using a

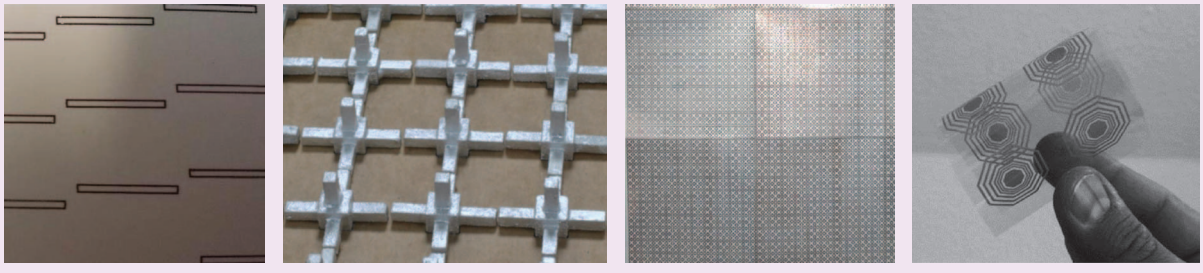

FIGURE 2. Examples of FSSs manufactured using conductive ink. (a) Skewed lattice frame dipoles printed on Printed Electronics Ltd. (PEL) paper [46], (b) a 3-D printed triple cross [47], (c) a broken convoluted square array printed on a PET substrate [48], and (d) an FSS-based, chipless RFID tag printed on PET foil [49].

professional embroidery digital machine. The authors highlighted the challenge in finding a highly conductive yarn that is physically compatible with the embroidering process. The band-reject FSS prototype produced poor results, with a transmission null slightly better than –10 dB and a roughly 250-MHz frequency offset. The authors theorized that such discrepancies could be attributed to the lossy nature of the yarn and felt; however, and as the reader may see in the "Main FSS Performance Variables" section, the conductive-yarn bulk conductivity and substrate permittivity have a significant impact on FSS performance. In [59], FSS square-loop prototypes were manufactured by using weaving and screen-printing methods. The woven sample used two picks of a silver-coated fiber and the base material was woven from 2/60-mercerized natural cotton with polyester sewing thread. The screen-printed FSS was produced using silver paste printed on a 100% polyester-base layer. The prototype was cured at 180 °C for 10 min. Both prototypes exhibited relatively good performance results. The authors of [60] produced three FSS prototypes using different methods and materials: one was produced using weaving with one pick of conducting yarn on a loom machine, one used embroidery with a polyester-spun yarn with stainless-steel fibers, and one was woven on a handloom with annealed bare copper wire. Of all the prototypes, the embroidered FSS produced the worst results, with the authors attributing the cause to the lower conductivity of the chosen yarn as well as the zig-zag stitching, which the authors assumed did not optimize current flow in the preferred directions.

Overall, textile-based FSSs can be a credible alternative to conventional manufacturing techniques. Taking into consideration that the production of this type of FSS can be integrated with established manufacturing procedures and associated with its general flexibility, softness, and overall visual tolerance by humans in indoor environments, this may be most useful for EM shielding at select frequency bands in building environments. If aesthetically integrated with curtains, the FSS can serve as both a visual and an EM barrier. An FSS designer should, however, take into consideration the impact that bending these flexible FSSs may have on the overall frequency response and, if so, compensate or account for such influences.

METAL

A characteristic common to all FSS designs is the requirement to have an electrically conductive element present in a specific arrangement within each unit cell. Instead of being partially composed of (or covered by) such conducting elements, an FSS might instead be entirely made of a metallic material. The authors of [62] and [63] proposed an FSS design that only has a nonconductive material as a support/fixation element. With this type of FSS, the electrical conductivity of the unit-cell elements is assured, since all metals exhibit good bulk conductivity values, a matter that is further addressed in the "Electrical Conductivity" section.

Figure 4 presents the FSS prototypes assembled by previously cited authors. The prototype of [62] consists of a periodic array of spring-resonator element structures. The unit cells are made of a thin aluminum wire (1 mm in diameter) wound into a helical spring resonator, and the 6 × 6 array is sandwiched between two foam substrates for structural support. By altering the height of the springs through applied mechanical pressure, a tunable frequency response is obtained. The authors of [63] presented a 3-D cylinder FSS in a dual-ring arrangement. The thought process consisted of expanding the classic 2-D ring-loop FSS to 3-D. By properly adjusting the radius of this dual-cylinder arrangement, the authors demonstrated a highly selective passband with one stopband on each side within a 1-MHz offset. Although the material used to assemble the prototype was not specified, a foam-based material was used for structural support.

The benefit of an all-metal FSS comes from the design's simplicity as well as its relatively easy manufacturing procedure. The structural integrity of a metal-based FSS is also significantly higher when compared to a PCB-based FSS or ink-covered designs. In the case of the pressure-tunable FSS in [62], the absence of discrete active elements or bias grids to achieve frequency tuning may prove useful in specific applications.

FLUID

Contrary to ink-based FSSs, liquid-tunable FSSs rely on the implied state of matter to achieve the desired performance

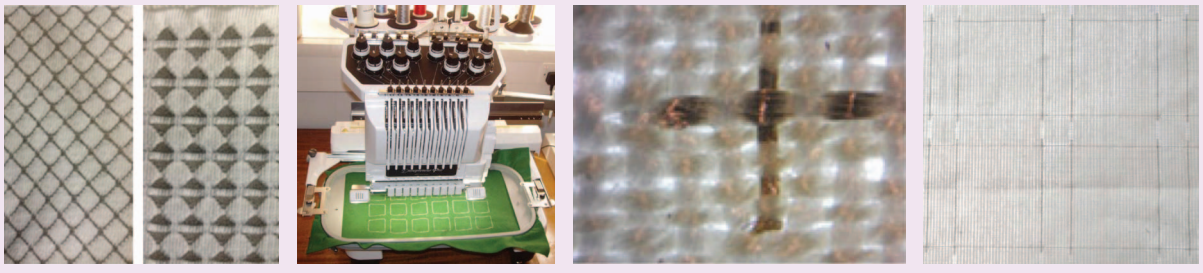

FIGURE 3. Examples of FSSs manufactured using textiles. (a) Two knitted patterns on polyester base yarn [57], (b) an embroidered pattern on felt cloth using a computerized machine [58], (c) details of contact points on the woven patterns on natural cotton [59], and (d) woven FSS square loops [60].

(a) (b)

FIGURE 4. Examples of FSSs manufactured using metals. (a) A helical spring resonator [62] and (b) a 3-D dual cylinder [63].

characteristics. Some FSS prototypes based on this property have been investigated, and some have displayed interesting results [64]–[67]. Two such publications, [66] and [67], used liquid metal to achieve frequency tuning, while the authors of [65] relied on liquid crystals.

The authors of [67] developed an FSS based on alternating volumes of liquid metal and dielectric fluid in periodically spaced tubes. Mercury (Hg) was the selected liquid metal, and mineral oil was the incompressible carrier fluid used to separate the Hg droplets. Polytetrafluoroethylene tubing was chosen because of its nonwetting surface properties. By means of a T-junction located within the pumping control circuit, specific liquid lengths for both metal and dielectric fluids should be possible and, consequently, achieve appropriate FSS tuning. The single-polarization manually controlled FSS prototype achieved a tuning range of 4.1–16.9 GHz, which equates to a 122% fractional bandwidth. Figure 5(a) depicts this FSS array design.

In [66], a similar approach to that of [67] was considered but with slight topology differences. Galistan, an eutectic alloy of gallium, indium, and tin was chosen as the liquid metal, flowing through Teflon tubes with air separating adjacent droplets. The FSS topology of [66] has the tube arrays embedded in a multilayer arrangement, with three different metal layers separated by two dielectric layers. The top and bottom metallic layers consist of square patches, while the middle layer is a metallic wire grid. The liquid-filled Teflon tubes are embedded on the two dielectric substrates that separate the metallic layers, as shown in Figure 5(b).

Tuning is achieved by carefully adjusting the liquid-metal-droplet length and its relative position with respect to the adjacent square patches. This adjustment modifies the capacitance value of each unit cell, which, if replicated across the entire FSS, will modify the overall FSS resonant frequency. The waveguide FSS prototype achieved a tuning range of 7.6 to 12.1 GHz; however, significant transmission losses at the higher-frequency tuned values were observed. The nontoxic liquid metal used in this prototype has the disadvantage of rapidly oxidizing when exposed to air [67], thus creating a gallium-oxide skin on the surface of the liquid, which is undesirable to large FSS arrays in an oxygenated environment.

The authors of [65] exploited the dielectric anisotropy of liquid crystals in D-band (110–170 GHz). The proposed FSS design consists of a two-layer array of dipole copper slots patterned on the inner surfaces of two supporting quartz wafers. The middle-layer cavity was filled with a proprietary liquid-crystal mixture. This mixture was biased through applied voltage between both copper-slot layers. This biasing rearranges the liquid-crystal molecules and, as a result, the relative permittivity of the overall liquid. As such, FSS frequency tuning is easily achieved by modifying the relative permittivity of a specific layer. The prototype exhibited a resonant-center frequency of 129–134 GHz for a maximum bias adjustment of 10 V. The authors of this prototype stated that, from the observed frequency response, this type of FSS should be better suited for a switching operation since it yields roughly 7 dB of dynamic range between 0- and 10-V bias states at 134 GHz.

A fluid-based FSS has been investigated with tuning capabilities through the manual or automatic adjustment of metallic/dielectric liquid ratios within unit cells. These techniques do not rely on electronic devices but, in some cases, are able to achieve significant tuning ranges, albeit for single polarization only, due to tubing-structural layouts. The liquid-crystal FSS of [65] was also included in this section despite its tuning being achieved by substrate permittivity modification.

MAIN FSS PERFORMANCE VARIABLES

The overall performance of an FSS, whether it is 2-D or 3-D, bandpass or bandstop, may be dictated by only a few physical elements and their specifications. As such, this section provides a performance analysis of the most relevant parameters, i.e., electrical bulk conductivity of the FSS conductive element and the relative permittivity of the dielectric element. This information should be basic acquired knowledge for researchers with a moderate FSS background. However, the authors consider that given the context of this article, such information should be presented.

ELECTRICAL CONDUCTIVITY

From the "FSS Materials" section, one may notice that common to all FSS manufacturing materials is the requirement of a good electrical conductive element. This element may be the copper sheets laminated onto dielectric substrates or the silver nanoparticles mixed in inks or embedded in textiles. Lower conductivity corresponds to higher resistivity to electric current flow, which, when applied to an FSS design context, translates to lower transmission/

reflection performance for bandpass/stop designs, respectively.

To assess the influence that electrical conductivity has on FSS performance, simulations were performed on the CST Microwave Studio Suite, where a canonical 2-D square loop and square slot etched from a FR4 PCB were chosen as demonstration examples. Both simulated designs have identical unit-cell dimensions with 35 μm of copper-sheet thickness on a 1.5-mm FR4 substrate, the results of which are shown in Figure 6. As one may observe from both plots, a conductivity value >50 kS/m should be targeted to obtain good FSS performance. Although these observations are only presented for 2-D PCB-based FSSs, they should remain valid for other 2-D or 3-D FSS manufacturing materials.

SUBSTRATE PERMITTIVITY

For all FSS designs that require the electrical conductive element to be physically supported by a dielectric material, the relative permittivity and thickness of the latter may cause a substantial impact on FSS performance. In the present study, the effect of dielectric loss (i.e., loss tangent) was considered to be negligible since its impact cannot be easily de-embedded from the S_{21} analysis. This circumstance is even further the case when the overall insertion loss of the FSS in the passband is <2 dB. To understand how the FSS frequency response is affected by such parameters, simulations were performed using a PCB-based FSS.

Figure 7 presents results for two different parameters, specifically relative permittivity (ε_r) and dielectric thickness (h). From Figure 7(a), we see that permittivity can significantly alter the resonance frequency for a fixed FSS unit-cell design. On the other hand, the dielectric thickness has a smaller impact on resonance-frequency offset, which is dependent on the permittivity value, as shown in Figure 7(b).

COMPARISON OF TECHNOLOGIES

For all of the previously mentioned possible FSS materials and their manufacturing technologies, one may attempt to compare and evaluate them for certain metrics, such as cost, unit-cell shape complexity, tuning or switching viability, physical flexibility, and the elements' electrical conductivity.

A cost comparison may be the most difficult idea to quantify because, depending on whether it is a one-off prototype or a large-volume order, prices will significantly vary for some, if not all of the aforementioned FSS materials. A PCB technique has the advantage of being widely available but is difficult to implement using flexible substrates; however, new techniques for flexible assemblies based on inkjet printing are becoming available [55], which will help overcome this problem in the future.

The unit-cell shape complexity is dictated by manufacturing procedures, i.e., high-precision machinery will be able to manufacture more complex FSS designs. Fluid-based FSS designs require some sort of tubing for the electrically conductive fluid (from examples depicted in the "Fluid" section) and, as such, should

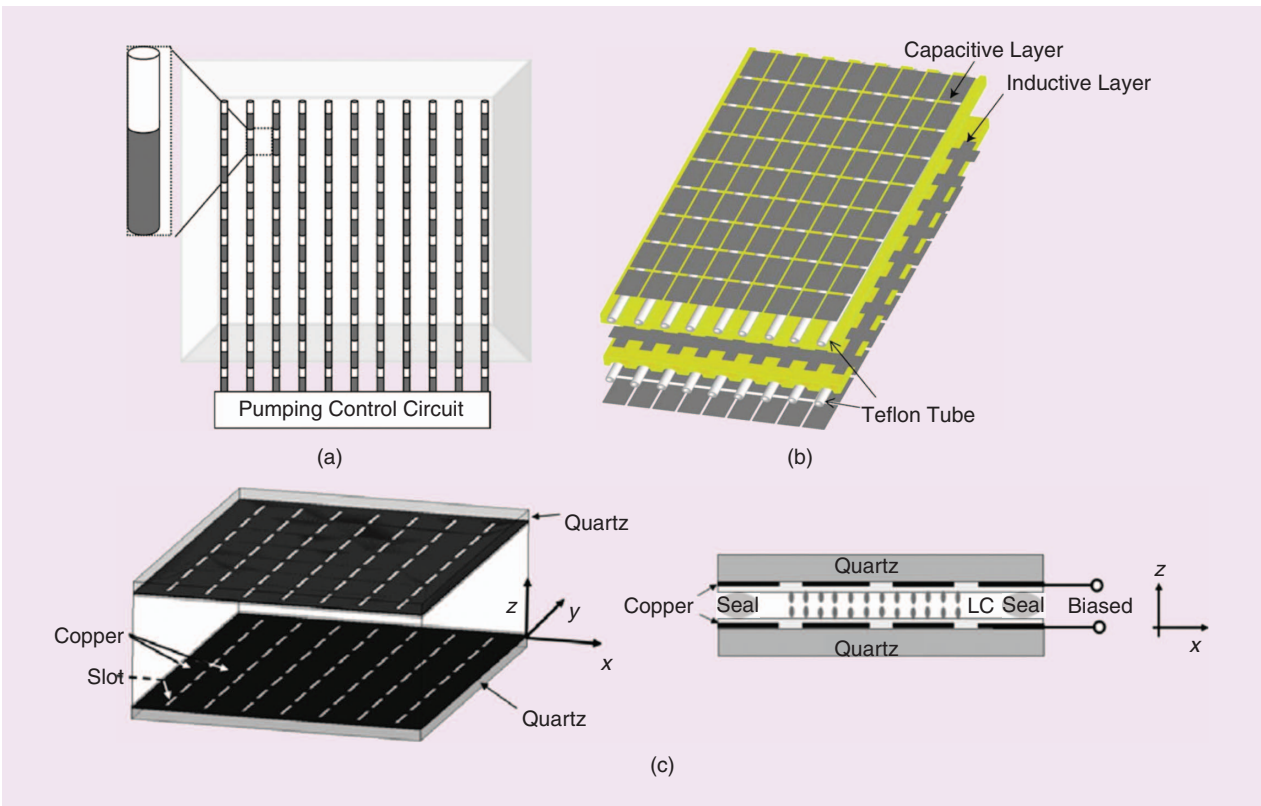

FIGURE 5. Examples of fluid-based FSSs. (a) Liquid metal on polytetrafluoroethylene tubing [67], (b) liquid metal on Teflon tubing sandwiched between three metallic layers [66], and (c) liquid crystal sandwiched between quartz wafers with copper film dipole slots [65].

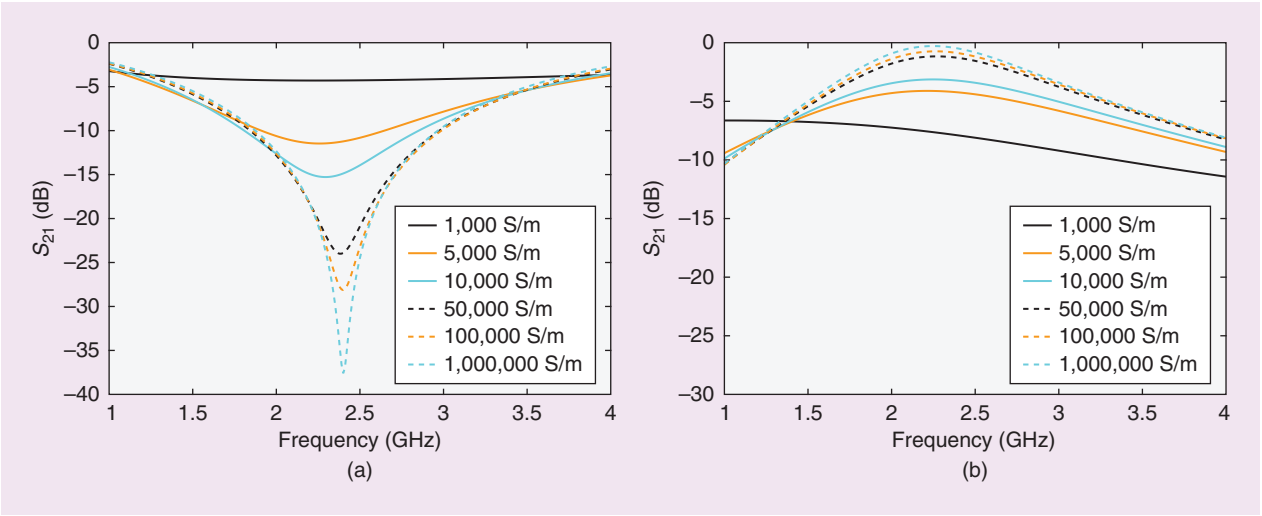

FIGURE 6. The bulk electrical conductivity influence on 2-D FSS performance. (a) A square loop and (b) a square slot.

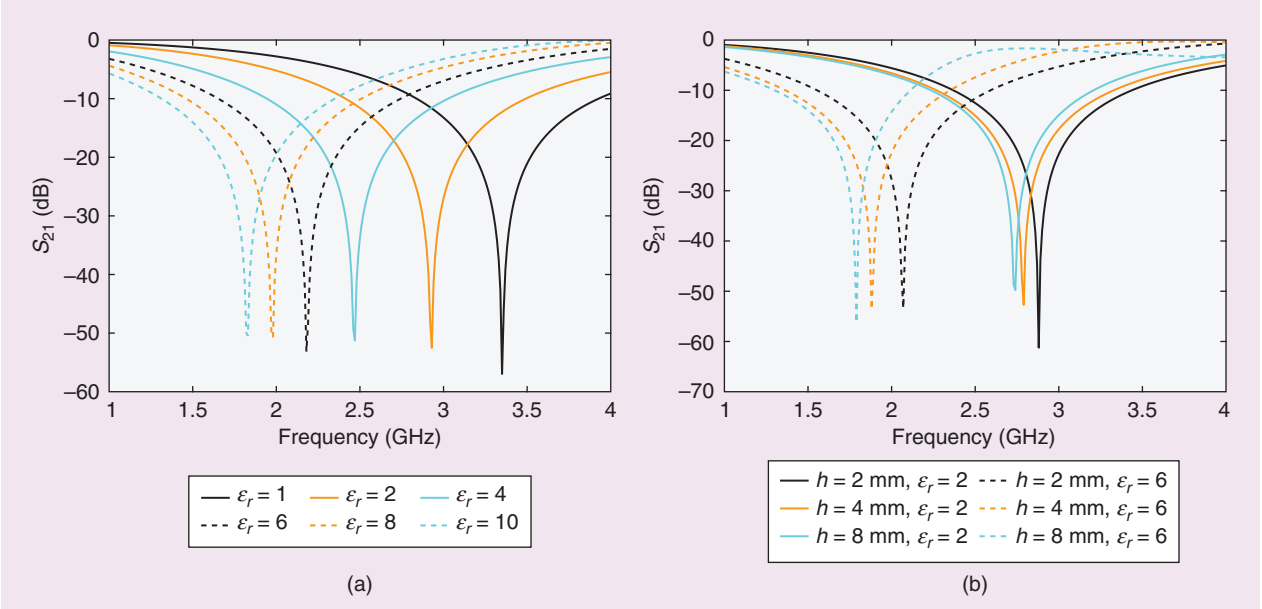

FIGURE 7. The dielectric influence on performance of a 2-D square-loop FSS design. (a) A relative permittivity parametric with thickness locked at 1.5 mm and (b) the thickness parametric for different permittivity values.

be the least-effective performer in this regard. PCBs and ink designs should, on the other hand, create more complex unit-cell designs.

In most situations, tuning and/or switching capability requires the inclusion of some discrete active element within the FSS unit cell, which, with appropriate biasing, will modify the overall frequency response. On PCB-based designs, common solutions include varactors, p-i-n diodes, or microelectromechanical systems. Introducing these elements may result in higher constraints where ink- or textile-based materials are concerned due to fixation and/or flexibility issues. The fluid-based designs presented in this article do, however, achieve tuning by controlling the ratio of electrically conductive fluid versus a dielectric medium.

Although most of the reported FSSs in this article are not mechanically flexible, certain applications may benefit from, or even require, flexibility in the FSS. PCB- and metallic-based designs have very low to no flexibility, while textile and some ink-based designs (depending on the substrate material) should allow for significant flexibility. Fluid-based FSSs may also achieve some flexibility if the unit cell is devised with flexible tubing. On the other hand, FSS performance may depend on the amount of exerted flexing, and, therefore, it must be assessed and accounted for in the FSS design stage.

The "Electrical Conductivity" section discussed the impact that the bulk

TABLE 1. THE ELECTRICAL CONDUCTIVITY OF VARIOUS ELEMENTS.

Material	Conductivity (S/m)
Silver	61 M
Copper	58 M
Aluminum	38 M
Stainless steel	1.1 M
Mercury	1 M
Conductive inks	2–20 M
Conductive textiles	2–100 k

electrical conductivity has on the overall FSS performance. With this in mind, some presented materials do have substantially better conductivity values than others. To more easily demonstrate this disparity, see Table 1. Silver, copper, and aluminum have the highest conductivity values but vary from a cost perspective. On PCB-based designs, the conductive element is a copper sheet, while silver in a nanoparticle form is most commonly mixed in inks or embedded in textiles, as mentioned previously. Both conductive textiles and inks may have different concentrations of silver as well as other metallic elements in their composition, hence the broad range of values presented in Table 1.

An FSS researcher should, therefore, identify the best solution for his or her project based on (but not limited to) the following metrics: cost-effective choice per unit cell, tuning possibility, shape complexity, mechanical flexibility, and electrical conductivity. These have to be properly evaluated based on the specific project requirements. For example, if the unit-cell approximate cost is not a limiting factor for the project, then PCB material should be a good candidate as it is widely available and it outperforms the other materials in almost all the other metrics.

CONCLUSIONS

This article reported on several approaches for manufacturing an FSS, highlighting some of the most relevant materials present in scientific literature. For each material, possible manufacturing methods were also identified. To the authors' knowledge, the approaches presented in this article were lacking in scientific literature and, therefore, should prove useful for both new and more experienced FSS researchers.

PCB-based FSSs are widely used in the scientific community as the preferred material for validation purposes, e.g., one-off or low-volume prototypes. Conductive inkjet printing with silver nanoparticle ink and R2R technology may be a viable commercial solution promoting high yield and cost efficiency.

Textile-based FSSs could be a viable solution for indoor environments, perhaps even in visually exposed implementations. On-body shielding is another possibility offered by conductive textiles. Conductive filaments/fabrics should be carefully selected since some reported solutions displayed low conductivity values, which negatively impacted the FSS prototype performance.

Metal-based FSSs are yet another alternative design approach in which good electrical conductivity is assured. Metal designs may, however, exhibit relatively high weight per unit cell compared to other approaches. Metal transforming in the machine industry is a very mature topic; therefore, high-yield commercial solutions should be possible.

Fluid-tunable FSS papers demonstrated interesting results, although these may require increased rigorous manufacturing and maintenance control when compared to other solutions. It was demonstrated that low electrical conductivity values severely limit FSS performance. Substrate properties may also have an effect on FSS characteristics but are manifested through a frequency offset, which is directly related to the relative permittivity and thickness of the substrate. Finally, the presented materials were also compared against each other for several important metrics, such as approximate cost, tuning possibility, mechanical flexibility, and electrical conductivity.

ACKNOWLEDGMENTS

This research was partially supported by the Portuguese Government, the Portuguese Foundation for Science and Technology, the Fundação para a Ciência e a Tecnologia with financial support provided under the QREN-POPH funding, and COMPETE 2020 under the project OptimizedWood (POCI-01-0247-FEDER-017867). This research was also supported by the Spanish Government, the Ministerio de Economía y Competitividad, the Secretaría de Estado de Investigación, the Desarrollo e Innovación, (Project TEC2014-55735-C03-3R), the AtlantTIC Research Center, and the European Regional Development Fund.

AUTHOR INFORMATION

David Ferreira (david.ferreira@co.it.pt) is with the Instituto de Telecomunicações, Leiria, Portugal. He is also with the University of Vigo, Spain. His research interests include frequency-selective surfaces and shielding techniques. He is a Student Member of the IEEE.

Rafael F.S. Caldeirinha (rafael.calderinha@ipleiria.pt) is head of the Antennas & Propagation Research Group at the Instituto de Telecomunicações, Leiria, Portugal, and a coordinating professor at the Polytechnic Institute of Leiria, Portugal. He is also with the University of South Wales, Treforest, United Kingdom. His research interests include the study of radio wave propagation through vegetation media, radio channel sounding and modeling and frequency selective surfaces, for applications at microwave and millimeter-wave frequencies. He is a Fellow of the Institution of Engineering and Technology and a Senior Member of the IEEE.

Iñigo Cuiñas (inhigo@uvigo.es) is a professor with the Department of Signal Theory and Communications and the dean of the School of Telecommunication Engineering at the Universidade de Vigo, Spain. His research interests include radio wave propagation in complex environments such as vegetation media, environmental aspects of radiofrequency systems, the development of techniques to reduce electromagnetic pollution, and using radio technologies in rural and vegetation environments. He is a Senior Member of the IEEE.

Telmo R. Fernandes (telmo.fernandes@ipleiria.pt) is an adjunct professor with the School of Technology and Management at the Polytechnic

Institute of Leiria, Portugal, and a researcher with the Antennas & Propagation Research Group at the Instituto de Telecomunicações, Leiria, Portugal. He is also with the University of South Wales, School of Engineering, Treforest, United Kingdom. His research interests include the study of radio wave propagation through vegetation media at microwave and millimeter-wave frequencies, frequency-selective surfaces, energy harvesting, and electromagnetic compatibility. He is a Senior Member of the IEEE.

REFERENCES

[1] B. A. Munk, *Frequency Selective Surfaces Theory and Design*. Hoboken, NJ: Wiley, 2000.

[2] G. V. Trentini, "Partially reflecting sheet arrays," *IRE Trans. Antennas Propag.*, vol. 4, no. 4, pp. 666–671, 1956.

[3] L. Henderson, B. Munk, S. Nichols and R. Brown, "Multilayer frequency sensitive surfaces of tripoles," in *Proc. Int. Symp. Antennas and Propagation Society*, 1982, pp. 459–462.

[4] E. A. Parker, S. M. A. Hamdy, and R. J. Langley, "Arrays of concentric rings as frequency selective surfaces," *Electron. Lett.*, vol. 17, no. 23, pp. 880–881, 1981. doi: 10.1049/el:19810614.

[5] E. A. Parker and S. M. A. Hamdy, "Rings as elements for frequency selective surfaces," *Electron. Lett.*, vol. 17, no. 17, pp. 612–614, 1981. doi: 10.1049/el:19810430.

[6] R. J. Langley and E. A. Parker, "Equivalent circuit model for arrays of square loops," *Electron. Lett.*, vol. 18, no. 7, pp. 294–296, 1982. doi: 10.1049/el:19820201.

[7] R. J. Langley and E. A. Parker, "Double-square frequency-selective surfaces and their equivalent circuit," *Electron. Lett.*, vol. 19, no. 17, pp. 675–677, 1983. doi: 10.1049/el:19830460.

[8] E. A. Parker, S. M. A. Hamdy, and R. J. Langley, "Modes of resonance of the Jerusalem cross in frequency-selective surfaces," *IEE Proc. H (Microw., Optics Antennas)*, vol. 130, no. 3, pp. 203–208, 1983.

[9] G. I. Kiani, L. G. Olsson, A. Karlsson, K. P. Esselle, and M. Nilsson, "Cross-dipole bandpass frequency selective surface for energy-saving glass used in buildings," *IEEE Trans. Antennas Propag.*, vol. 59, no. 2, pp. 520–525, 2011.

[10] M. Raspopoulos and S. Stavrou, "Frequency selective buildings through frequency selective surfaces," *IEEE Trans. Antennas Propag.*, vol. 59, no. 8, pp. 2998–3005, 2011.

[11] T. Smith, U. Gothelf, O. S. Kim, and O. Breinbjerg, "An FSS-backed 20/30 GHz circularly polarized reflectarray for a shared aperture L- and Ka-band satellite communication antenna," *IEEE Trans. Antennas Propag.*, vol. 62, no. 2, pp. 661–668, 2014.

[12] R. Nair and R. Jha, "Electromagnetic design and performance analysis of airborne radomes: Trends and perspectives," *IEEE Antennas Propag. Mag.*, vol. 56, no. 4, pp. 276–298, 2014.

[13] D. Ferreira, L. Sismeiro, A. Ferreira, R. F. S. Caldeirinha, T. R. Fernandes, and I. Cuiñas, "Hybrid FSS and rectenna design for wireless power harvesting," *IEEE Trans. Antennas Propag.*, vol. 64, no. 5, pp. 2038–2042, 2016.

[14] B. Sanz-Izquierdo and E. A. Parker, "Dual polarized reconfigurable frequency selective surfaces," *IEEE Trans. Antennas Propag.*, vol. 62, no. 2, pp. 764–771, 2014.

[15] B. Liang, B. Sanz-Izquierdo, E. Parker, and J. Batchelor, "Cylindrical slot FSS configuration for beam-switching applications," *IEEE Trans. Antennas Propag.*, vol. 63, no. 1, pp. 166–173, 2015.

[16] A. Edalati and T. Denidni, "High-gain reconfigurable sectoral antenna using an active cylindrical FSS structure," *IEEE Trans. Antennas Propag.*, vol. 59, no. 7, pp. 2464–2472, 2011.

[17] R. J. Mittra, C. H. Chan, and T. A. Cwik, "Techniques for analyzing frequency selective surfaces: A review," *Proc. IEEE*, vol. 76, no. 12, pp. 1593–1614, 1988.

[18] T. K. Wu, Ed., *Frequency Selective Surface and Grid Array*. Hoboken, NJ: Wiley, 1995.

[19] T. K. Chang, R. J. Langley, and E. A. Parker, "An active square loop frequency selective surface," *IEEE Microw. Guided Wave Lett.*, vol. 3, no. 10, pp. 387–388, 1993.

[20] B. Philips, E. A. Parker, and R. J. Langley, "Active FSS in an experimental horn antenna switchable between two beamwidths," *Electron. Lett.*, vol. 31, no. 1, pp. 1–2, 1995. doi: 10.1049/el:19950007.

[21] T. K. Chang, R. J. Langley, and E. A. Parker, "Active frequency selective surfaces," *IEE Proc.—Microw., Antennas Propag.*, vol. 143, no. 1, pp. 62–66, 1996. doi: 10.1049/ip-map:19960115.

[22] J. C. Vardaxoglou, P. Y. Lau, and M. Kearney, "Frequency selective surface from optically excited semiconductor on a substrate," *Electron. Lett.*, vol. 34, no. 6, pp. 570–571, 1998. doi:10.1049/el:19980409.

[23] B. M. Cahill and E. A. Parker, "Field switching in an enclosure with active FSS screen," *Electron. Lett.*, vol. 37, no. 4, pp. 244–245, 2001. doi: 10.1049/el:20010159.

[24] I. Gil, J. Bonache, J. García-García, F. Martín and R. Marqués, "Tunable split rings resonators for reconfigurable metamaterial transmission lines," in *Proc. European Microwave Conf.*, 2005, p. 908.

[25] G. I. Kiani, K. P. Esselle, A. R. Weily, and K. L. Ford, "Active frequency selective surface using PIN diode," in *Proc. IEEE Int. Symp. Antennas and Propagation*, 2007, pp. 4525–4528.

[26] G. I. Kiani, K. L. Ford, L. G. Olsson, K. P. Esselle, and C. J. Panagamuwa, "Switchable frequency selective surface for reconfigurable electromagnetic architecture of buildings," *IEEE Trans. Antennas Propag.*, vol. 58, no. 2, pp. 581–584, 2010.

[27] M. Moallem and K. Sarabandi, "A single-layer metamaterial-based polarizer and bandpass frequency selective surface with an adjacent transmission zero," in *Proc. IEEE Int. Symp. Antennas and Propagation*, 2011, pp. 2649–2652.

[28] B. Sanz-Izquierdo, E. A. Parker, and J. C. Batchelor, "Switchable frequency selective slot arrays," *IEEE Trans. Antennas Propag.*, vol. 59, no. 7, pp. 2728–2731, 2011.

[29] P. S. Taylor, E. A. Parker, and J. C. Batchelor, "An active annular ring frequency selective surface," *IEEE Trans. Antennas Propag.*, vol. 59, no. 9, pp. 3265–3271, 2011.

[30] M. Li and N. Behdad, "A third-order bandpass frequency selective surface with a tunable transmission null," *IEEE Trans. Antennas Propag.*, vol. 60, no. 4, pp. 2109–2113, 2012.

[31] Q. Chen, J. Jiang, X. Xu, L. Zhang, L. Miao and S. Bie, "A thin and broadband tunable radar absorber using active frequency selective surface," in *Proc. IEEE Int. Symp. Antennas and Propagation Society*, 2012, pp. 1–2.

[32] L. Zhang, G. Yang, Q. Wu, and J. Hua, "A novel active frequency selective surface with wideband tuning range for EMC purpose," *IEEE Trans. Magn.*, vol. 48, no. 11, pp. 4534–4537, 2012.

[33] F. Deng, X. Yi, and W. Wu, "Design and performance of a double-layer miniaturized-element frequency selective surface," *IEEE Antennas Wireless Propag. Lett.*, vol. 12, pp. 721–724, May 2013.

[34] R. Natarajan, M. Kanagasabai, S. Baisakhiya, R. Sivasamy, S. Palaniswamy, and J. K. Pakkathillam, "A compact frequency selective surface with stable response for WLAN applications," *IEEE Antennas Wireless Propag. Lett.*, vol. 12, pp. 718–720, May 2013.

[35] A. K. Rashid, B. Li, and Z. Shen, "An overview of three-dimensional frequency-selective structures," *IEEE Antennas Propag. Mag.*, vol. 56, no. 3, pp. 43–67, 2014.

[36] X. G. Huang, Z. Shen, Q. Y. Feng, and B. Li, "Tunable 3-D bandpass frequency-selective structure with wide tuning range," *IEEE Trans. Antennas Propag.*, vol. 63, no. 7, pp. 3297–3301, 2015.

[37] D. Ferreira, R. F. S. Caldeirinha, I. Cuiñas, and T. R. Fernandes, "Square loop and slot frequency selective surfaces study for equivalent circuit model optimization," *IEEE Trans. Antennas Propag.*, vol. 63, no. 9, pp. 3947–3955, 2015.

[38] S. Sheikh, "Miniaturized-element frequency-selective surfaces based on the transparent element to a specific polarization," *IEEE Antennas Wireless Propag. Lett.*, vol. 15, pp. 1661–1664, Jan. 2016.

[39] D. Ferreira, I. Cuiñas, R. F. S. Caldeirinha, and T. R. Fernandes, "Dual-band single-layer quarter ring frequency selective surface for Wi-Fi applications," *IET Microw., Antennas Propag.*, vol. 10, no. 4, pp. 435–441, 2016. doi: 10.1049/iet-map.2015.0641.

[40] A. Ebrahimi, Z. Shen, W. Withayachumnankul, S. F. Al-Sarawi, and D. Abbott, "Varactor-tunable second-order bandpass frequency-selective surface with embedded bias network," *IEEE Trans. Antennas Propag.*, vol. 64, no. 5, pp. 1672–1680, 2016.

[41] A. A. Omar and Z. Chen, "Multiband high-order bandstop 3-D frequency-selective structures," *IEEE Trans. Antennas Propag.*, vol. 64, no. 6, pp. 2217–2226, 2016.

[42] D. S. Wang, P. Zhao, and C. Chan, "Design and analysis of a high-selectivity frequency-selective surface at 60 GHz," *IEEE Trans. Microw. Theory Techn.*, vol. 64, no. 6, pp. 1694–1703, 2016.

[43] M. Gao, S. Abadi, and N. Behdad, "A dual-band, inductively coupled miniaturized-element frequency selective surface with higher order bandpass response," *IEEE Trans. Antennas Propag.*, vol. 64, no. 8, pp. 3729–3734, 2016.

[44] P. Zhao, Z. Zong, W. Wu, and D. Fang, "A convoluted structure for miniaturized frequency selective surface and its equivalent circuit for optimization design," *IEEE Trans. Antennas Propag.*, vol. 64, no. 7, pp. 2963–2970, 2016.

[45] A. Al-Sheikh and Z. Shen, "Design of wideband bandstop frequency-selective structures using stacked parallel strip line arrays," *IEEE Trans. Antennas Propag.*, vol. 64, no. 8, pp. 3401–3409, 2016.

[46] B. M. Turki, E. A. Parker, S. Wünscher, U. S. Schubert, R. Saunders, V. Sanchez-Romaguera, M. A. Ziai, S. G. Yeates, and J. C. Batchelor, "Significant factors in the inkjet manufacture of frequency-selective surfaces," *IEEE Trans. Compon. Packag. Manuf. Technol.*, vol. 6, no. 6, pp. 933–940, 2016.

[47] B. Sanz-Izquierdo and E. A. Parker, "3D printing technique for fabrication of frequency selective structures for built environment," *Electron. Letters*, vol. 49, no. 18, p. 1117, 2013. doi: 10.1049/el.2013.2256.

[48] J. A. Miller, J. C. Batchelor and E. A. Parker, "FSS printed using conducting ink," in *Proc. IEEE Int. Symp. Antennas and Propagation Society*, 2010, pp. 1–4.
[49] D. Betancourt, K. Haase, A. Hübler, and F. Ellinger, "Bending and folding effect study of flexible, fully-printed and late-stage codified octagonal chipless RFID tags," *IEEE Trans. Antennas Propag.*, vol. 64, no. 7, pp. 2815–2823, 2016.
[50] G. I. Kiani, A. Karlsson, L. Olsson and K. P. Esselle, "Glass characterization for designing frequency selective surfaces to improve transmission through energy saving glass windows," in *Proc. Asia-Pacific Microwave Conf.*, 2007, pp. 1–4.
[51] O. Sushko, M. Pigeon, T. Kreouzis, C. Parini, R. Donna, and R. Dubrovka, "Low-cost Inkjet-printed FSS Band-pass Filters for 100 and 300 GHz," in *Proc. European Conf. Antennas and Propagation (EuCAP)*, 2016, pp. 1–3.
[52] S. N. Zabri, R. Cahill, G. Conway, and A. Schuchinsky, "Inkjet printing of resistively loaded FSS for microwave absorbers," *Electron. Lett.*, vol. 51, no. 13, pp. 999–1001, 2015. doi: 10.1049/el.2015.0696.
[53] B. M. Turki, E. A. Parker, R. Saunders, J. Wheeler, S. G. Yeates and J. C. Batchelor, "Deficiencies in printed FSS intended for application in smart buildings," in *Proc. IEEE Int. Symp. Antennas and Propagation & USNC/URSI Nat. Radio Science Meeting*, 2015, pp. 320–321.
[54] H. J. Song, J. H. Schaffner, K. A. Son and J. S. Moon, "Optically transparent Ku-band silver nanowire frequency selective surface on glass substrate," in *Proc. IEEE Int. Symp. Antennas and Propagation Society (APSURSI)*, 2014, pp. 2100–2101.
[55] W. Whittow, A. Chauraya, J. Vardaxoglou, Y. Li, R. Torah, K. Yang, S. Beeby, and J. Tudo, "Inkjet-printed microstrip patch antennas realized on textile for wearable applications," *IEEE Antennas Wireless Propag. Lett.*, vol. 13, pp. 71–74, 2014.
[56] C. Hertleer, H. Rogier, L. Vallozzi, and L. V. Langenhove, "A textile antenna for off-body communication integrated into protective clothing for firefighters," *IEEE Trans. Antennas Propag.*, vol. 57, no. 4, pp. 919–925, 2009.
[57] A. Tennant, W. Hurley, and T. Dias, "Experimental knitted, textile frequency selective surfaces," *Electron. Lett.*, vol. 48, no. 22, pp. 1386–1388, 2012. doi: 10.1049/el.2012.3005.
[58] A. Chauraya, R. Seager, W. Whittow, S. Zhang, and Y. Vardaxoglou, "Embroidered frequency selective surfaces on textiles for wearable applications," in *Proc. Loughborough Antennas and Propagation Conf. (LAPC)*, 2013, pp. 388–391.
[59] R. D. Seager, A. Chauraya, J. Bowman, M. Broughton, R. Philpott, and N. Nimkulrat, "Fabric-based frequency selective surfaces using weaving and screen printing," *Electron. Lett.*, vol. 49, no. 24, pp. 1507–1509, 2013. doi: 10.1049/el.2013.2314.
[60] R.D. Seager, A. Chauraya, J. Bowman, M. Broughton and N. Nimkulra, "Fabrication of fabric-based frequency selective surfaces (FSS)," in *Proc. European Conf. Antennas and Propagation (EuCAP)*, 2014, pp. 1978–1980.
[61] S. Zhang, R. Seager, A. Chauraya, W. Whittow and Y. Vardaxoglou, "Textile manufacturing techniques in RF devices," in *Proc. Loughborough Antennas and Propagation Conf. (LAPC)*, 2014, pp. 182–186.
[62] S. N. Azemi, K. Ghorbani, and W. S. T. Rowe, "A reconfigurable FSS using a spring resonator element," *IEEE Antennas Wireless Propag. Lett.*, vol. 12, pp. 781–784, June 2013.
[63] W. S. T. Rowe, A. R. As-Saber, S. N. Azemi and K. Ghorbani, "3-D frequency selective surfaces with highly selective responses," in *Proc. Loughborough Antennas and Propagation Conf. (LAPC)*, 2015.
[64] A. C. de C. Lima, E. A. Parker, and R. J. Langley, "Tunable frequency selective surface using liquid substrate," *IEE Electron. Lett*, vol. 30, no. 4, pp. 281–282, 1994. doi: 10.1049/el:19940232.
[65] W. Hu, R. Dickie, R. Cahill, H. Gamble, Y. Ismail, V. Fusco, D. Linton, N. Grant, and S. Rea, "Liquid crystal tunable mm-wave frequency selective surface," *IEEE Microw. Compon. Lett.*, vol. 17, no. 9, pp. 667–669, 2007.
[66] M. Li, B. Yu, and N. Behdad, "Liquid-tunable frequency selective surfaces," *IEEE Microw. Compon. Lett.*, vol. 20, no. 8, pp. 423–425, 2010.
[67] B. J. Lei, A. Zamora, T. F. Chun, A. T. Ohta, and W. A. Shiroma, "A wideband, pressure-driven, liquid-tunable frequency selective surface," *IEEE Microw. Compon. Lett.*, vol. 21, no. 9, pp. 465–467, 2011.